An Efficient Test Methodology for Combustion Engine Testing: Methods for Increasing Measurement Quality and Validity at the Engine Test Bench

2017-01-0604
Published 03/28/2017

Christian Friedrich
MAN Diesel & Turbo SE

Yves Compera
Technical University of Munich

Matthias Auer and Gunnar Stiesch
MAN Diesel & Turbo SE

Georg Wachtmeister
Technical University of Munich

CITATION: Friedrich, C., Compera, Y., Auer, M., Stiesch, G. et al., "An Efficient Test Methodology for Combustion Engine Testing: Methods for Increasing Measurement Quality and Validity at the Engine Test Bench," SAE Technical Paper 2017-01-0604, 2017, doi:10.4271/2017-01-0604.

Abstract

Improving fuel efficiency while meeting relevant emission limits set by emissions legislation is among the main objectives of engine development. Simultaneously the development costs and development time have to be steadily reduced. For these reasons, the high demands in terms of quality and validity of measurements at the engine test bench are continuously rising.

This paper will present a new methodology for efficient testing of an industrial combustion engine in order to improve the process of decision making for combustion-relevant component setups. The methodology includes various modules for increasing measurement quality and validity. Modules like stationary point detection to determine steady state engine behavior, signal quality checks to monitor the signal quality of chosen measurement signals and plausibility checks to evaluate physical relations between several measurement signals ensure a high measurement quality over all measurements. For increasing measurement validity, engine setting parameters are permanently monitored to ensure exact and consistent engine adjustments according to the test plan. Furthermore, embedded 0D engine simulations are used to correct undesired setting parameter deviations in order to create a consistent data base used for model-based optimization (DoE) and combustion-relevant component decisions.

The methodology was verified by a measurement campaign carried out at an industrial engine. The new methodology is reducing potential incorrect measurements that have to be repeated. In addition, it ensures that only valid measurements are taken for model-based techniques (DoE) that have been 0D-corrected if necessary. Test bench time can be shortened, leading to a reduction in and better utilization of development costs as well.

Introduction

Reducing fuel consumption and emissions is one of the main objectives in the engine development. This paper focusses on the development of industrial engines for marine and power plant applications. Considering the long service lives of industrial engines, even small improvements in fuel consumption and engine efficiency within a range of 0.5% rigorously affect operation costs and environmental pollution. Furthermore, stricter regulations on the emission of carbon dioxide inside and outside Europe have to be met by modern industrial engines. Therefore, even minor potential and improvements have to be exploited in terms of engine development.

Since modern engine test benches are equipped with complex measurement instrumentations and an extensive number of sensors and actuators that all interact with one another, a high level of effort is required to ensure accurate measurements. Because of their significant influence on post processing in terms of further decisions and counteractions in the process of engine development, erroneous measurements must be avoided as far as possible. Therefore, a high measurement quality has to be ensured to evaluate different engine configurations. Nevertheless, permanently accurate measurements cannot be ensured. The appearance of random errors has to be taken into account at any time. Moreover, measurement errors caused by incorrect manual inputs cannot be completely avoided either. Hence, methods must be utilized to reduce the number of invalid measurements by detecting potential errors before measurements are recorded.

The technology of modern combustion engines is becoming more and more complex in order to increase flexibility. Modern industrial engines are equipped with technologies like common rail (CR) injection systems, dual fuel combustion processes and two-stage turbocharging, leading to higher parameter numbers that have to be observed during engine tests. The higher number of parameters increases the number of measurements needed to identify optimal engine settings regarding engine hardware and software parameters.

On the contrary, the number of measurements is limited by the test bench costs and available test bench time. The overall costs of an engine test bench can be split into:

- Preparation costs
- Operation costs
- Consumption costs
- Dead time costs
- Post processing costs

Consumption and dead time costs dominate in terms of industrial engine measurements. Due to their big size, heavy weight and high power output, industrial engines have higher total fuel oil consumptions and require much longer stabilization times (e.g. for stabilization of exhaust gas temperatures) to reach steady state engine operation. For these reasons only twenty to thirty measurements can be taken in one day, permitting only moderate experimental designs.

Figure 1 shows a simplified fictitious example illustrating the complexity of the process of decision making in terms of combustion-relevant hardware setups. Within the example, the engine efficiencies depending on the start of injection for two different injection nozzle geometries of a diesel engine with common rail injection system are compared. Nozzle geometry A and B have different injection angulars ψ.

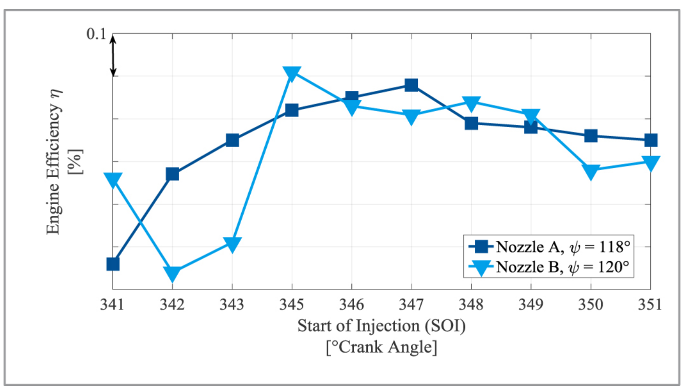

Figure 1. Fictitious engine efficiency for various injection timings for two different injection nozzle geometries.

As can be seen in the diagram, the different injection angulars only lead to very minor differences in engine efficiency. Without any further information given by supporting tools, an appropriated decision for one of the nozzle geometries is nearly impossible. Since the differences in engine efficiency are very small, it is essential for measurement errors to be avoided at all times. As already mentioned above, it is impossible to ensure that measurements are always accurate. Therefore, correcting invalid measurements, e.g. due to incorrect manual inputs at the engine test bench, where possible would create a better data base for the decision making.

In summary, the demands in terms of high measurement quality and validity continue to rise at the engine test bench. A reliable process of decision making for combustion-relevant engine hardware setups can only be ensured by combining assisting methods and tools to create an innovative methodology. Various publications like [1, 2, 3, 4] have presented methods for increasing measurement quality in terms of engine development in recent years. Data-based and physical approaches have been used and implemented at engine test benches to avoid erroneous measurements during engine testing. In contrast to these studies the developed methodology focusses on hardware setup independent methods and embeds 0D engine simulations. The overall methodology and the combined methods and tools used will be presented in detail within this paper.

After a description of the overall methodology, the methods for increasing measurement quality and measurement validity will be presented in detail. Furthermore, the measurement campaign carried out at an industrial engine test bench in order to validate the methodology will be described. With the help of the measurement campaign, the main achievements in utilizing the developed methodology will be shown and discussed critically. A short summary and conclusion will be given at the end of the paper.

Overall Methodology

The main objective of the new methodology is to increase the measurement quality and validity at the engine test bench of industrial engines. In this chapter the methods developed, tools and their application will be presented. Figure 2 gives an overview of the methodology's workflow.

The whole workflow starts with a preparation phase. As mentioned in the introduction, there is a conflict in objectives between the limited number of possible measurements (costs and duration) and the validity of those measurements taken. The fewer measurements there are, the harder it is to ensure high measurement validity. To limit the scope of measurements, design of experiments (DoE) has been introduced to combustion development of industrial engines in recent years [5]. Utilizing DoE, statistical test plans (e.g. d-optimal or space filling) are set up which will be measured at the engine test bench.

In the second phase of the methodology, the measurements are run at the test bench. In past years, test engineers and test bench operators were responsible for all tasks relating to the taking of measurements. They had to monitor all sensors, detect steady state engine operation and check the measurement plausibility as well. Since statistical DoE test plans are used, verifying the measurements and estimating the changes of the operating values for the next measurement is almost impossible. The error potential of measurements is increasing. To support the test bench operators and reduce their responsibilities to an appropriate extent, methods for increasing measurement quality were introduced. The new methodology combines a stationary point detection, signal quality and plausibility checks. Steady state engine operation will be detected automatically by monitoring the gradients of the chosen measurement signals. The determination of signals' gradients is the most practical and reliable method for a steady state detection (SSD) in engine test applications [6]. Long waiting periods to guarantee steady state behavior become redundant when a SSD is utilized. Measurements can be started directly when steadiness is detected. Signal quality checks ensure an overall high quality of the chosen measurement signals by observing the statistical signal to noise ratio [1]. Plausibility checks are the third method for increasing measurement quality. Physical relationships between measurement signals such as energy and mass conservation can be evaluated. Utilizing all three methods allows potential measurement errors to be detected before erroneous measurements are taken. This also allows measurements to become more comparable and reliable.

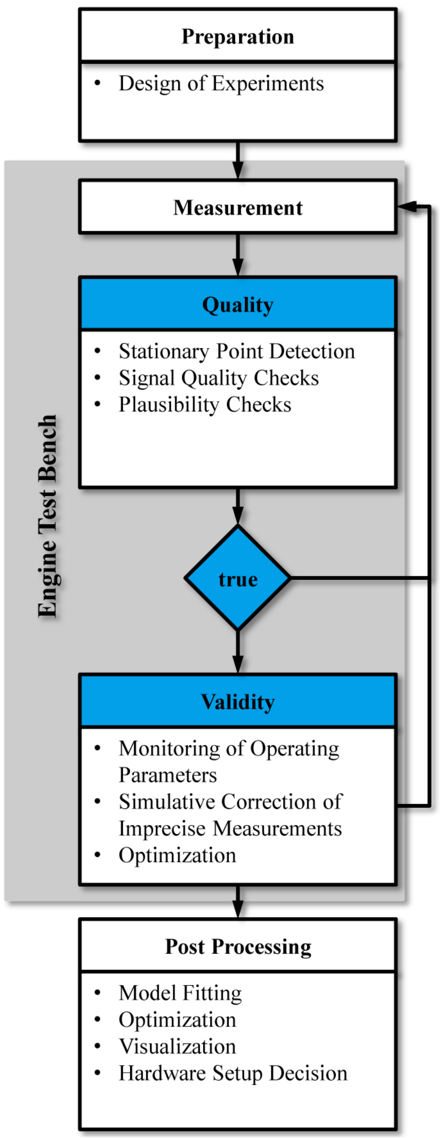

Figure 2. General overview of the methodology's workflow.

The methods for increasing measurement quality are followed by methods for increasing measurement validity. Therefore, all relevant sensors will be monitored systematically. For each sensor or operating value respectively, threshold values and critical gradient can be set to avoid sensor drifts. A fuzzy designer continuously checks the accuracy of the operating values. If critical deviations appear, an error will be reported. Since threshold values and critical gradients are set by test engineers, their subjective knowledge can be used in mathematical algorithms. Furthermore, a 0D engine simulation is integrated to improve the measurement validity. Predictions of the engine behavior depending on the engine setting parameters utilizing a proper combustion model are attempted. Small measurement errors resulting from minor mistakes in manual input values should be correctable and predictions of pressure curves and NO_x emissions for the next operating point should be possible as well.

After all measurements have been recorded at the engine test bench, post processing is performed. Data-driven regression models are fitted by the measured data. These models are used for numerical optimizations and plotting tradeoffs for test evaluation purposes. Decisions regarding combustion-relevant hardware setups will be made utilizing the results of numerical optimizations.

In the following chapters, the methods and tools mentioned, which are combined in the overall methodology, will be presented in more detail.

Methods for Increasing Measurement Quality

The methods for increasing measurement quality used within this study can be divided into three different modules. The first module is a stationary point detection that is able to detect whether the engine has reached steady state operation or not. The second module, the signal quality checks, monitors the signal quality of chosen measurement signals. Last but not least, the plausibility checks module checks physical relationships between several measurement signals that have to been fulfilled. A detailed description of all three modules and some fundamental basics of the methods used will be given in the next three sections.

Stationary Point Detection

Most measurements recorded at engine test benches in terms of engine development are taken during steady state engine operation [6, 7, 8]. When engine inputs (e.g. injection timing or rail pressure) are adjusted, it takes some time before all measurement signals have reached stationary behavior. In recent years, steady state operation has often been evaluated by the persons operating the engine. To avoid possible subjective misjudgments, various steady state detection algorithms have been investigated [6, 9, 10, 11, 12]. Furthermore, modern test bench automation systems allow constant stabilization times to be defined before measurements are taken during automated test run procedures of engines [13, 14].

Similar to [6], in this study a steady state detection based on the evaluation of gradients of several measurement signals is used. The gradient $g_{y_i}(t)$ of any measurement signal y_i is given by the first derivative of the measurement signal with respect to the time t:

$$g_{y_i}(\mathrm{t}) = \frac{\partial y_i(t)}{\partial t} \ . \tag{1}$$

A signal can be evaluated as stationary if the determined derivative $\frac{\partial y_i(t)}{\partial t}$ is lower in comparison to a defined limit value $l_{g_{y_i}}$:

$$\frac{\partial y_i(t)}{\partial t} \leq l_{g_{y_i}} \ .$$

(2)

In case of a noisy raw measurement signal, the first derivative of the signal is hard to compute [6]. Therefore, a moving average filter is applied to smooth those noisy measurement signals. The moving average $m_{y_i}^n(t)$ at the time t for n sample values is given by:

$$m_{y_i}^n(t) = \frac{1}{n}\sum_{j=0}^{n-1} y_i(t-j) \ .$$

(3)

Once the moving average has been computed from n samples, the gradients are determined by the derivative of the moving average values with respect to the time:

$$g_{m_{y_i}^n}(\mathrm{t}) = \frac{\partial m_{y_i}^n(t)}{\partial t} \ .$$

(4)

As with equation (2), the measurement signal can be evaluated as stationary if the gradient $g_{m_{y_i}^n}(t)$ is lower than a limit value $l_{g_{m_{y_i}^n}}$:

$$\frac{\partial m_{y_i}^n(t)}{\partial t} \leq l_{g_{m_{y_i}^n}} \ .$$

(5)

The functional principle of the stationary point detection using the example of the exhaust gas temperature of a diesel engine is shown in Figure 3. The adjustment of the start of injection of a diesel engine has a strong influence on the exhaust gas temperature. Adjusting the start of injection to an earlier timing leads to a lower exhaust gas temperature. However, it takes several minutes until the exhaust gas temperature value has reached its final value. The upper diagram of Figure 3 shows the raw exhaust gas temperature values $\vartheta_{Exhaust}(t)$ over the time t. By three and a half minutes, the start of injection is adjusted to an earlier timing leading to a decrease in the exhaust gas temperature. In the diagram in the middle, the raw exhaust gas temperature signal is smoothed from noise by computing the moving average $m_{\vartheta_{Exhaust}}(t)$ out of 30 samples taken with a frequency of 1 Hz according to equation (3). From these moving averages, the gradients $g_{m_{\vartheta_{Exhaust}}}(t)$ are determined according to equation (4). The resulting gradients $g_{m_{\vartheta_{Exhaust}}}(t)$ over the time t are depicted in the lower diagram. The limit values for the exhaust gas temperatures are plotted in the lower diagram as well. As is shown, the gradients increase above the limit values directly after the start of injection is adjusted. Only after seven minutes are the gradients below the limit values again. Hence, in this example it takes approximately three and a half minutes for the exhaust gas temperature to reach steady state behavior.

The stationary point detection can be implemented for various chosen measurement signals. This allows those signals to be selected that have an overall slow behavior (e.g. temperatures) influencing the stabilization time of the whole engine significantly.

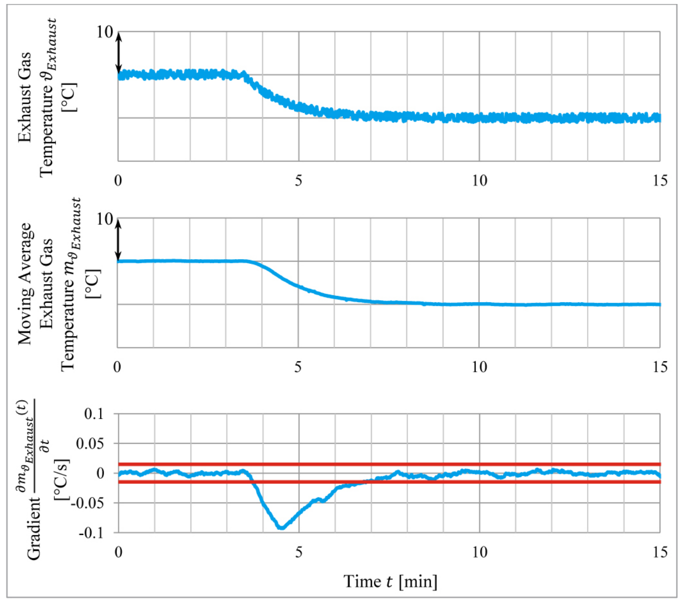

Figure 3. Stationary point detection using the example of the exhaust gas temperature $\vartheta_{Exhaust}$ after the start of injection of a diesel engine is adjusted to an earlier timing.

For test evaluation purposes, a quality criterion is derived from the stationary point detection of all selected signals. If a signal y_i is rated to be stationary, the single stationary value SSV_i of this signal is assigned as one (SSV_i=1). If the signal is not stationary, the single stationary value is assigned as zero (SSV_i=0). The total stationary value (TSV) for all n selected signals is calculated as the mean value of all single stationary values:

$$TSV = \frac{1}{n}\sum_{i=1}^{n} SSV_i \ .$$

(6)

The total stationary value TSV can have values between zero and one, where the recording of a measurement can be recommended for total stationary values exceeding a defined limit.

Signal Quality Checks

According to [1], the statistical signal to noise ratio (SNR) is an appropriate measure for determining the signal quality of the chosen measurement signals at engine test benches. Recalling the moving average $m_{y_i}^n(t)$ of any signal y_i of n samples according to equation (3) and utilizing the moving standard deviation $\sigma_{y_i}^n(t)$:

$$\sigma_{y_i}^n(t) = \sqrt{\frac{1}{n-1}\sum_{j=0}^{n-1}\left(y_i(t-j) - m_{y_i}^n(t-j)\right)^2} \ .$$

(7)

the SNR_{y_i} is given by:

$$SNR_{y_i} = 20 \cdot lg\left(\frac{m_{y_i}^n(t)}{\sigma_{y_i}^n(t)}\right).$$

(8)

Since the logarithm to the base 10 is applied in the equation above, the SNR has the unit decibel. Commonly the SNR takes values within a range of 20 to 60 dB. The higher the value, the better the signal quality. Hence, the signal quality can be rated good when the SNR_{y_i} is higher in comparison to a defined limit value $l_{SNR_{y_i}}$:

$$SNR_{y_i} \geq l_{SNR_{y_i}} \; . \tag{9}$$

For example, Figure 4 depicts the signal quality check of the engine speed signal $n_{Engine}(t)$ at two different load points. The upper diagram plots the raw signal of the engine speed over the time t. Since the engine speed controller is more precise for higher engine speeds, the engine speed signal shows different deviations from the desired speed value at each load point. The second diagram shows the moving average of the engine speed signal $m_{n_{Engine}}(t)$. Using this moving average and the moving standard deviation $\sigma_{n_{Engine}}(t)$ the signal to noise ratio $SNR_{n_{Engine}}(t)$ is computed and plotted in the lower diagram. The limit value $l_{SNR_{n_{Engine}}}$ is 45 dB. While the signal to noise ratio is above this limit value for the higher engine speed load point, it decreases below the limit for the lower engine speed point.

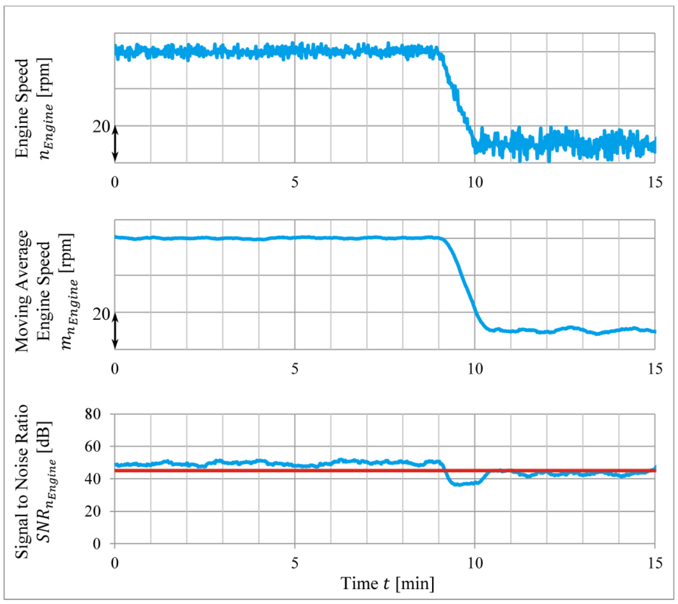

Figure 4. Signal quality check using the example of the engine speed n_{Engine} at two different load points of an engine.

Similar to the total stationary value TSV (see equation (6)), a total signal quality value $TSQV$ is introduced, combining the results of all signal quality checks performed for several measurement signals. The single signal quality value $SSQV_i$ of any measurement signal y_i will be assigned as one ($SSQV_i = 1$) if the signal quality is rated good. Otherwise the single signal quality value is set to zero ($SSQV_i = 0$) for a poorly-rated signal quality. Similar to equation (6), for n selected signal quality checks the total signal quality value of a measurement can be computed as:

$$TSQV = \frac{1}{n} \sum_{i=1}^{n} SSQV_i \; . \tag{10}$$

As with the total stationary value, the total signal quality value can take values between zero and one. However, recording measurements is only recommended for values above a defined limit to ensure good signal qualities for all measurement signals analyzed.

Plausibility Checks

Plausibility checks monitor elementary physical relationships between measurement signals. The plausibility checks that will be introduced in this section are similar to those presented in studies [1, 2, 3, 4] regarding measurement plausibility in recent years. Since the engine hardware setup in terms of combustion development purposes changes very often, general plausibility criteria independent from the engine hardware setup have been pursued within this study. An overview of the plausibility criteria used in this study is given in Table 1.

Table 1. Overview of plausibility criteria used within this study.

Criteria	**Description**
Sensor Checks	Checks whether the measurement value given by any sensor is within the specified measurement range of the sensor
Set Value / Actual Value Comparisons	Comparison of set values and actual values of any test bed controllers (e.g. charge air temperature controller)
Inequations	Examination of fundamental inequations between temperatures and pressures (e.g. cooling water temperature at engine inlet is lower than cooling water temperature at engine outlet)
Air to Fuel Ratios	Comparison of air to fuel ratios computed in different ways (e.g. comparison of air to fuel ratio determined by air and fuel mass flow measurement with air to fuel ratio determined by the Brettscheider equation published in [15])
Balances	Examination of physical balances such as energy, carbon and oxygen mass flow balances of the engine (conservation of energy and mass)

As an example of all plausibility criteria, the oxygen mass flow balance of the engine will be explained in this paper in more detail. The law of mass conservation presumes that the oxygen mass flow $\dot{m}_{O_2,Engine,in}$ into the engine is equal to oxygen mass flow coming out $\dot{m}_{O_2,Engine,out}$:

$$\dot{m}_{O_2,Engine,in} = \dot{m}_{O_2,Engine,out} \; . \tag{11}$$

The oxygen mass flow into the engine can be computed using the air mass flow $\dot{m}_{Air}$, water mass flow $\dot{m}_{H_2O,Air}$ from the absolute air humidity H_a, fuel mass flow $\dot{m}_{Fuel}$ and the oxygen mass fraction of each substance ($\xi_{O_2,Air}$, ξ_{O_2,H_2O}, $\xi_{O_2,Fuel}$) into the engine:

$$\begin{aligned} \dot{m}_{O_2,Engine,in} &= \dot{m}_{Air} \cdot \xi_{O_2,Air} + \dot{m}_{H_2O,Air} \cdot \xi_{O_2,H_2O} + \cdots \\ &\quad + \dot{m}_{Fuel} \cdot \xi_{O_2,Fuel} \\ &= \dot{m}_{Air} \cdot \xi_{O_2,Air} + \dot{m}_{Air} \cdot H_a \cdot \xi_{O_2,H_2O} + \cdots \\ &\quad + \dot{m}_{Fuel} \cdot \xi_{O_2,Fuel} \; . \end{aligned} \tag{12}$$

Taking the mass flows of carbon dioxide $\dot{m}_{CO_2}$, carbon monoxide $\dot{m}_{CO}$, nitrogen oxides $\dot{m}_{NO_x}$, water $\dot{m}_{H_2O,Exhaust}$ and oxygen $\dot{m}_{O_2}$ in the exhaust gas multiplied by the oxygen mass fraction of each substance (ξ_{O_2,CO_2}, $\xi_{O_2,CO}$, ξ_{O_2,NO_x}, ξ_{O_2,H_2O}), the oxygen mass flow out of the engine can be determined:

$$\begin{aligned}\dot{m}_{O_2,Engine,out} &= \dot{m}_{CO_2} \cdot \xi_{O_2,CO_2} + \dot{m}_{CO} \cdot \xi_{O_2,CO} + \cdots \\ &+ \dot{m}_{NO_x} \cdot \xi_{O_2,NO_x} + \cdots \\ &+ \dot{m}_{H_2O,Exhaust} \cdot \xi_{O_2,H_2O} + \dot{m}_{O_2} \ .\end{aligned} \tag{13}$$

Since the law of mass conservation has to be met, the deviations between oxygen mass flow into the engine and oxygen mass flow out of the engine should be as small as possible. A deviation limit $l_{O_2,Balance}$ can be introduced to restrict the deviations to an acceptable level:

$$\left|\dot{m}_{O_2,Engine,in} - \dot{m}_{O_2,Engine,out}\right| \leq l_{O_2,Balance} \ . \tag{14}$$

The measurement point shown in Figure 5 has a slightly lower oxygen mass flow out of the engine than the mass flow into the engine. The deviation is still below the deviation limit, so the plausibility criterion is fulfilled. A possible reason for small deviations could be seen in the blow by (leakage of the air-fuel mixture or of combustion gases between a piston and the cylinder wall into the crankcase) that is not taken into account in the balance equations.

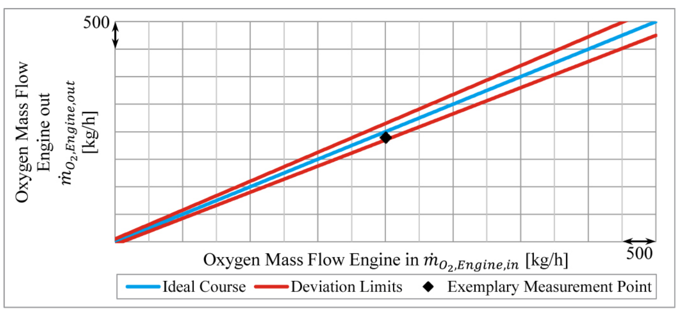

Figure 5. Plausibility check using the example of the oxygen mass balance of a combustion engine.

For test evaluation purposes, a total plausibility value *TPV* of a measurement, taking all used plausibility criteria, is introduced. Similar to the stationary point detection and the signal quality checks, a single plausibility value of one ($SPV_i = 1$) is assigned if any plausibility criterion is fulfilled. Otherwise it is assigned as zero ($SPV_i = 0$). By using specific weights, the importance of the plausibility criteria can be controlled. The following weights w_i have been defined in this study:

- w_i=1 for a low weight
- w_i=3 for a medium weight
- w_i=5 for a high weight

Using these weights, the total plausibility value is given by the weighted mean of *n* plausibility criteria and their single plausibility values SPV_i:

$$TPV = \frac{\sum_{i=1}^{n}(w_i \cdot SPV_i)}{\sum_{i=1}^{n} w_i} \ . \tag{15}$$

A recommendation to record measurements is only made when total plausibility values exceed a defined limit.

Methods for Increasing Measurement Validity

Monitoring of Engine Setting Parameters

Recalling Figure 2, the methods for increasing measurement quality described previously are followed by methods to ensure measurement validity. In order to avoid invalid input values or wrong adjustment controls according to the test plans, the input parameters of each operating point are monitored permanently. The method of this monitoring is depicted schematically in Figure 6.

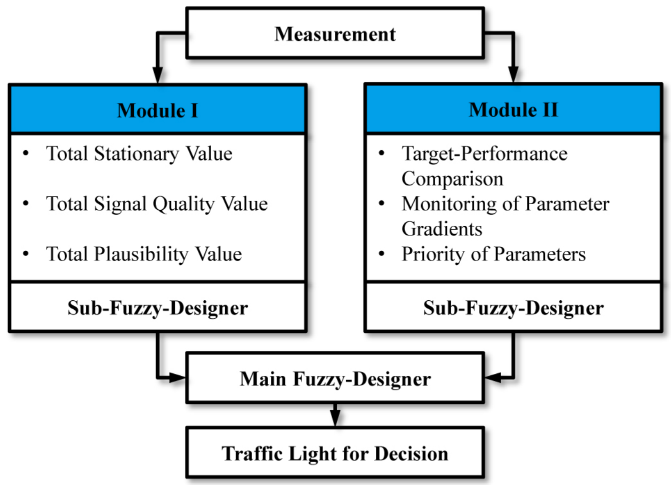

Figure 6. Overview of the method using the fuzzy-designer.

Generally, the monitoring is divided into two different modules. In Module I the stationary point value, the total signal quality value, and the total plausibility value calculated previously are evaluated. They all take numeric values between zero and one. The measurement quality rises with increasing values. However, the challenge is to identify the critical limit values reliably for all kinds of engine types and at each engine test bench. Against this background the experience of the test bench operators in combination with the first sub fuzzy logic designer can be used to define the limit range for each value. Furthermore, the values can be prioritized by the fuzzy designer as well. In Module II the other sub fuzzy logic designer is used to monitor the target-performance comparison, the gradient, and the priority of the entire engine setting parameters automatically. Subsequently, the main fuzzy logic designer assesses the results from the sub fuzzy logical designer to make a final decision in terms of a traffic light's signal.

Fuzzy Logic Designer

The idea of turning the test bench expert's subjective knowledge and their many years of experience into a mathematical algorithm can be realized by means of the fuzzy logic method. Fuzzy logic (FL) provides the automatic evaluation of sensor data and the linguistic description of a system while taking advantage of domain knowledge [16]. Figure 7 shows the FL Designer. Generally, the FL maps inputs into outputs. Crisp sets allow only full membership or no membership at all, whereas fuzzy sets allow partial membership [17].

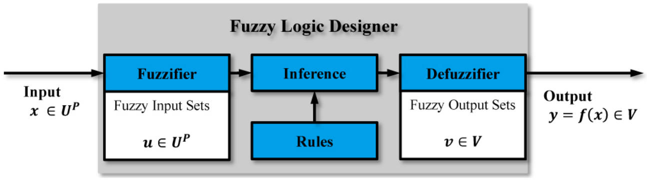

Figure 7. Fuzzy Designer according to [17]

In a crisp set, membership or non-membership of element x in set A is described by a characteristic function $\mu_A(x)$, where $\mu_A(x) = 1$ *if* $x \in A$ and $\mu_A(x) = 0$ *if* $x \notin A$ [17]. Fuzzy set theory extends this concept by defining partial membership. The most commonly used shapes for membership functions are triangular, trapezoidal, piecewise linear and Gaussian. In this paper triangular and Gaussian functions have been used. Fuzzy sets represent linguistic labels like *large, heavy, low, medium, high, tall* etc. [17]. So a given element can be a member of more than one fuzzy set at a time. An example of the membership function of the charge air temperature deviation is given by Figure 8.

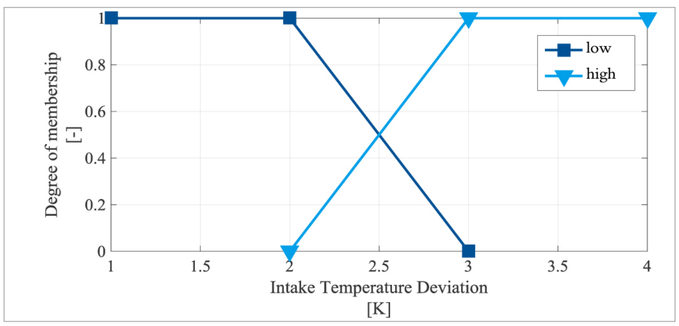

Figure 8. Example of a membership function.

A fuzzy set A in U may be represented as a set of ordered pairs. Each pair consists of a generic element x and its grade of membership function: $A = \{(x, \mu_A(x)), x \notin U\}$ [17]. In the first step, the fuzzifier maps the numbers into fuzzy sets. This is necessary because in the next step rules in terms of linguistic variables must be taken into account. The rules are provided by the engine test bench experts and are given as IF-THEN statements (e.g. IF the temperature deviation is high THEN display an error). The transfer from the linguistic variable versus the numerical value of a variable is given by the fuzzifier mentioned before. In the next step, the fuzzy inference, the nonlinear mapping from a given input to an output using fuzzy logic (fuzzy rules) will be defined. The degree to which the antecedent is satisfied for each rule is determined by the fuzzy inference [17]. Fuzzy operators are applied to obtain only one number which displays the result if the antecedent of a given rule has more than one clause [17]. In this paper the Mamdani-type of inference systems is used because it is the most common and recommended for this application by [16, 17]. Last, the defuzzifier maps output fuzzy sets into a crisp number.

Integration of 0D Engine Simulation

Despite the great effort taken as mentioned, it is impossible to rule out some invalid setting parameter deviations. With this in mind, the 0D engine simulation is integrated in the evaluation of the engine test. The main goal is to subsequently correct the invalid measurements by 0D engine simulation.

The 0D engine simulation solves the conservation equation of mass and energy in consideration of the equation of state in the thermodynamic system. It is composed by an intake and exhaust container and the cylinder volume. There, mass and enthalpy through scavenging, through blow-by flows and heat flows through combustion, wall heat losses, and the volume change of the piston movement can be exchanged. The boundary condition for the scavenging is the state of the gas straight before the intake and straight after the exhaust valve. The thermodynamic system and its relevant simulation parameters are shown in Figure 9.

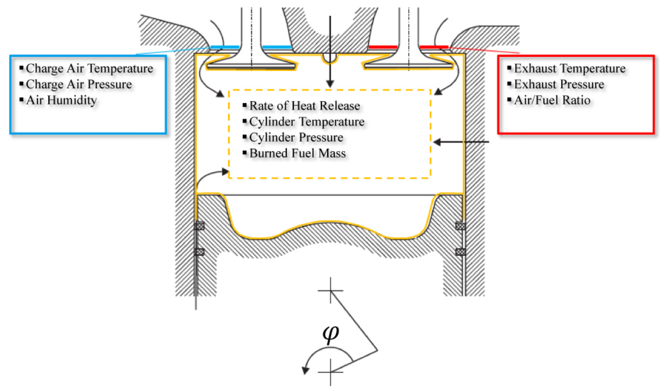

Figure 9. Definition of the thermodynamic system.

0D engine simulation is a very efficient means of performing parametric studies since it quickly computes the main quantities relevant to the engine design and operating conditions. Therefore, a large number of empirical, semi-phenomenological and approved correlations have been developed in the past. This paper focuses on the prediction of the rate of heat release (ROHR).

In this paper the integration of the 0D engine simulation was examined on an industrial diesel engine with CR injection (see next chapter). Eilts` quasi-steady ROHR model which only needs one calibration parameter is used [18]. His ROHR model is based on the theory of single phase stationary turbulent jets, respectively diffusion flames [18]. In [18] the good correspondence between measured and calculated performance data as well as pressure and ROHR curves is depicted. This ROHR model was chosen because of its advantage that only one parameter must be calibrated. In contrast, other ROHR models named in literature, like [19, 20, 21] need divers calibration parameters. Using Eilts` ROHR model the calibration can be done with only one measurement. After calibrating the ROHR model the 0D engine simulation clearly gives the response of a parameter variation. Even though, if the absolute simulation result does not perfectly match the measurement, the delta value of the simulated parameter variation gives a significant prediction of the parameter changing effect as a first approximation. This proceeding tends to improve the accuracy of the inaccurate measurements carried out. At the same time, the number of re-measurements can be reduced. Furthermore, the simulation of the next operating point by means of the pressure, temperature, ROHR, and emission curves supports the test bench operators.

Since this proceeding requires its own ROHR model for specific engine types, a listing of approved models is given in Table 2. These models can be easily exchanged in the used 0D simulation software of the Institute of Internal Combustion Engines of the Technical University of Munich.

Table 2. Specification of the used combustion model for the particular combustion process.

Engine Type	**Combustion Process Model**
CR Diesel Engine	Eilts' Model, [18]
Spark Plug Lean Gas Engine	Auer's Model, [22, 23]
Pre-Chamber Lean Gas Engine	Auer's Model, [22, 23]
Dual Fuel Diesel Gas Engine	Walther's Model, [24]

Thus the ROHR models presented can be applied to the most common engine types, the methodology is usable in a wide range. On this basis, the application of further emission models like NO_x according to [25, 26, 27, 28] and soot according to [29, 30] is possible.

Application of the Methodology

Experimental Setup

All measurements for methodology validation were taken from a four-stroke industrial diesel engine test bench. The 12V configuration of the engine is depicted in Figure 10.

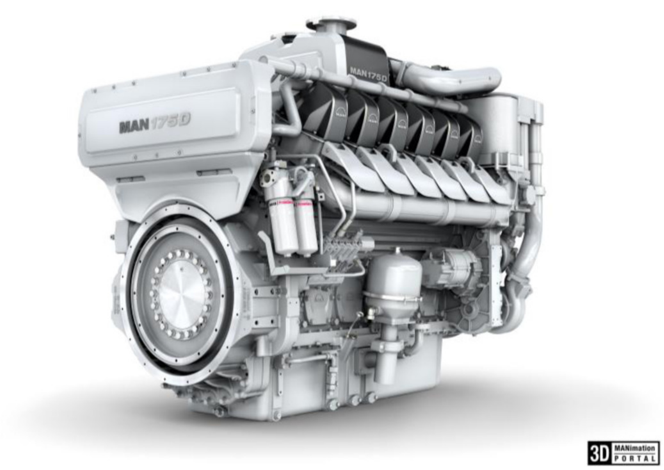

Figure 10. MAN Diesel & Turbo four-stroke industrial diesel engine 12V175D.

This diesel engine can cover various applications. Beside mechanical propulsion, genset and diesel-electric drive applications are scenarios in which the engine is typically used. Within this study, however, only the genset application at constant engine speed is taken into account. The engine is equipped with a common rail (CR) injection system allowing the adjustment of injection pressures and timings independently at any load point. Further specifications of the engine can be found in Table 3.

An extensive amount of measuring equipment is installed at the engine test bench. Beside standard measuring devices to observe temperatures, pressures and media flows, special measurement systems, e.g. a pressure indicating system, exhaust gas analyzers and a torque measuring flange are available as well. The indicating system delivers high-resolution measurements of charge air, exhaust and combustion pressures. Exhaust gas analyzers determine NO_x, CO_2, CO and HC fractions and soot in the exhaust gas.

Table 3. Specification of the MAN Diesel & Turbo 175D industrial diesel engine.

Application	Genset
Fuel	EN590
Engine speed	1,500 or 1,800 rpm
Engine power per cylinder	135 kW @ 1,500 rpm 160 kW @ 1,800 rpm
Dimensions LxHxW (12V)	2,645 x 2,135 x 1,485 mm
Weight (12V)	8,200 kg
Injection system	CR injection system
Turbocharger	Single-stage turbocharger

Measurement Campaign

The measurement campaign covered two different aspects. On the one hand, three different engine hardware setups were investigated and compared. On the other hand, special measurements were taken among all the other measurements to verify the methods developed regarding measurement quality and validity.

Measurements for Performance Comparison of Different Hardware Setups

Measurements with three different engine hardware setups were taken, varying in the injector nozzle geometry. All measurements of each hardware setup were performed according to a combination of d-optimal and space filling DoE test plans in order to limit the scope of measurements and to allow a numerical determination of optimal engine parameter settings with the help of data-driven regression models. Within all statistical test plans, the following engine setting parameters were varied:

- Engine load (load points 25%, 50%, 75% and 100%)
- Rail pressure
- Injection timing

As an example, Figure 11 shows the statistical test plan for one of the three engine hardware setups investigated. All statistical test plans include a total number of 30 test points. The test point distribution of all three test plans for the engine hardware setups is very similar. However, slight differences exist since the ranges of the engine setting parameters, leading to no limit violations (e.g. exceedance of maximum cylinder pressure or maximum exhaust gas temperature), needed to be changed. As is shown below, measurements are only taken at four load points that are relevant for the emission cycle.

Based on the recorded measurements, regression models have been fitted for the following engine outputs:

- Specific fuel oil consumption
- Specific NO_x emissions
- Soot
- Cylinder pressure
- Exhaust gas temperature

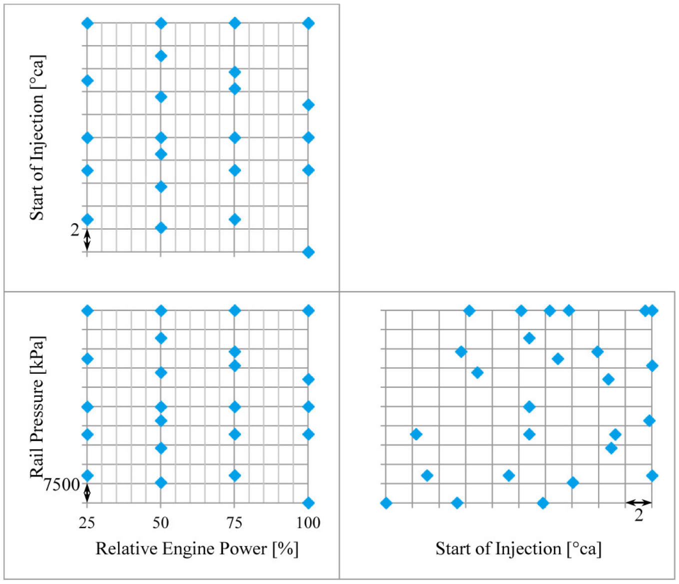

Figure 11. Statistical test plan for one engine hardware setup.

To ensure high quality in the data-driven regression models, a model committee similar to [1] was built for each specified engine output, containing the following model approaches:

- Polynomials
- Radial basis function networks
- Gaussian process models

The best model for each engine output is chosen by comparing selected statistical criteria for model evaluation (see [1]). Once the best models had been chosen from the model committees, numerical optimizations for each hardware setup were performed in order to determine optimal parameter settings for rail pressure and start of injection at each emission-relevant load point. The main objective for the optimization was to minimize the specific fuel oil consumption, while also meeting the following optimization constraints:

- Possible parameter settings only within the boundaries given by the test plan
- NO_x-cycle value below limit
- NO_x below 150% of NO_x-cycle limit for every single load point
- Soot below visibility
- Cylinder pressure below the mechanical limit
- Exhaust gas temperature below the material limit

Thereafter, the optimization results of each engine hardware setup were compared in order to choose the best hardware setup for the given boundary conditions.

Measurements for Tool and Method Validation Purposes

The tools for increasing measurement quality and validity have been implemented at the engine test bench so that they can be validated. Figure 12 shows a screenshot of the software for increasing measurement quality.

Figure 12. Screenshot of the software implemented for increasing measurement quality.

Some special measurements were taken during the measurement campaign. One aim of these special measurements was to validate whether or not erroneous measurements can be corrected by 0D engine simulations. Measurements at non-steady engine operation and measurements with incorrect manual input values for charge air pressure and temperature have been recorded during the measurement campaign to investigate this matter.

Another aim of the special measurements was to analyze the effect of the methods for increasing measurement quality regarding reduction of erroneous measurements. Therefore, the measurements of the first engine hardware setup were taken without paying attention to the results of the stationary point detection, signal quality and plausibility checks. For all other measurements, these tools were used intensively before any measurements at the engine test bench were recorded.

Results

Reduction in Number of Measurements

In the past, full factorial test plans have usually been used for hardware setup investigations. Keeping the four different load points and varying rail pressure and start of injection to three steps, a full factorial test plan would comprise 36 test points. Hence, the statistical test plan including 30 measurements reduces the measurement amount by about 17%.

The results regarding reduction in erroneous measurements by using the stationary point detection, signal quality and plausibility checks are given in Table 4.

Table 4. Reduction of erroneous measurements utilizing the methods for increasing measurement quality.

	Hardware Setup 1	Hardware Setup 2	Hardware Setup 3
Measurements [-]	30	30	30
Methods for increa-sing quality used?	No	Yes	Yes
Erroneous Measurements [-]	4	1	1
Erroneous Measurements [%]	13.3	3.3	3.3

There are several reasons why measurements were rated invalid. Some of the measurements did not reach stationary engine behavior because the measurement was recorded too early. In addition, for some of the measurements the set value versus actual value comparisons were not fulfilled (e.g. charge air temperature deviations higher than one degree Celsius and lube oil pressure deviations higher than 100 kPa).

Summarizing Table 4, the percentage of erroneous measurements within the scope of this study can be reduced by approximately 10%. Where four invalid measurements were recorded with hardware setup one, in each of the other hardware setups, only one measurement was identified as erroneous. Hence, the utilization of the methods led to a noteworthy reduction in invalid measurements. Fewer measurements therefore have to be retaken at the engine test bench, reducing operation costs and shortening development time significantly.

Performance Comparison and Hardware Setup Decision

Based on the measurements taken from the test bench according to statistical test plans, data-driven regression models were fitted and used for numerical optimization for each hardware setup (see the "Measurement Campaign" subchapter). The optimization was carried out as a cycle optimization considering the defined NO_x-cycle limit value. The results of these numerical optimizations, taking into account various constraints regarding emission and mechanical or material limits, are shown in Figure 13.

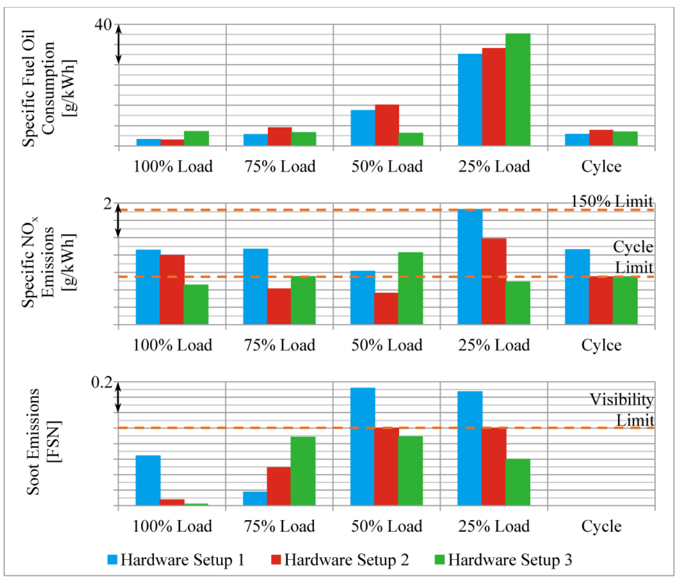

Figure 13. Numerical optimization results for all three engine hardware setups investigated.

As is shown, only the results for specific fuel oil consumption, specific NO_x emissions and soot are given. First of all, any engine hardware setup has to fulfil the requirements regarding emissions legislations. Thus, NO_x emissions and soot have to be below the defined limits.

The diagram in the middle shows the specific NO_x emissions at each load point and the NO_x-cycle value calculated from these values. The NO_x-cycle value has to be below the cycle limit including an engineering margin (lower dashed line) and the values at each individual load point must not exceed 150% of the respective cycle limit according to IMO regulations [31]. Since hardware setup one exceeds the permitted NO_x-cycle it can be excluded from the hardware setup decision. Furthermore, the soot at 50% and 25% engine load of hardware setup one also exceed the visibility limit value (see lower diagram), confirming the decision against hardware setup one, although this setup does display the best specific fuel oil consumptions (see upper diagram).

The engine hardware setups two and three meet all requirements regarding NO_x emissions, soot, maximum cylinder pressure and maximum exhaust gas temperature. For this reason, the combustion-relevant hardware decision can be made, using the results of the specific fuel oil consumption in the upper diagram. Depending on the load profile required by customers, one of the setups investigated is more suitable than the other. A customer's engine running almost at 50% engine load should be equipped with hardware setup three since it has significant lower specific fuel oil consumption at 50% engine load than hardware setup two. Hardware setup two would be the better choice for customers running the engine almost at 100% engine load, because of the lower specific fuel oil consumption at this load.

Correction of Invalid Measurements

Keeping 100% engine load the charge air temperature, charge air pressure, rail pressure, and the start of injection (SOI) were varied. The detailed parameter variation is given in Table 5. It is important to mention that the charge air pressure was varied with a constant pressure ratio between charge air and exhaust. Without this parameter variation pretending invalid measurements the results should not change. Consequently, the correction of invalid parameters by simulation must lead to a constant curve for each target parameter. In order to verify the results for the classical field of tension between engine power, efficiency and emission, the maximum cylinder pressure, the engine efficiency and the NO_x emissions were taken into account.

Table 5. Special measurements (Listing of the parameter variation).

Measurement No. [-]	$\Delta T_{Charge\ Air}$ [%]	$\Delta p_{Charge\ Air}$ [%]	Δp_{Rail} [%]	ΔSOI [°ca]
1	0	0	0	0
2	1.1	0	0	0
3	1.2	0	0	0
4	2.3	0	0	0
5	2.6	3	0	0
6	2.3	6	0	0
7	2.3	-3	0	0
8	2.3	-6	0	0
9	2.3	-6	0	0.5
10	2.3	-6	2.5	0
11	2.3	-6	0	0

Figure 14 shows, by way of example, the correction of the maximum cylinder pressure by 0D engine simulation, represented by the blue curve. The dark blue line shows the target curve if the measurement had no defects. This curve is constant with the value of the first reference measurement. It becomes obvious that the following measurements deviate from that curve due to the slight variations listed in Table 5. The approach of the simulative correction is the following. Two 0D engine simulations are calculated. The first one is given input values such as charge air temperature, charge air pressure etc. from the measurement (actual simulation) and the second receives target values from the test plan as input. The difference or delta between those two simulation results yields to the target-performance comparison. It is assumed that this comparison can be applied for the measurement as well. Therefore, the delta of the target-performance comparison is subtracted from the measurement. Thus, the change in result due to the slight input parameter change becomes visible when this delta is subtracted from the curve measured (see blue curve).

Though, the actual simulation (dashed black curve) only matches the curve measured in a range of ± 5% this approach can be justified since more the proper mapping through simulation is emphasized rather than matching the exact measurement values. The gray curve represents the target simulation with the set points of the test plan and the injected mass measured as input values. This curve is not constant though the input values are all the same in this example. The reason is that the injection duration, and thereby the injected fuel mass, will be controlled by the engine control unit (ECU). If the cylinder pressure changes the injected mass has to be adapted in order to operate with constant load. Hence, the correction is only justified for small parameter variations and is not 100% accurate.

The regulation of the charge air temperature incurs long waiting periods at the test bench. It is conceivable to reduce the control accuracy and criteria of the stationary point detection and thereby the waiting period if the deviation can be corrected by simulation. For this reason small temperature deviations were examined but it can be seen that a slight temperature deviation does not significantly affect the maximum pressure. The measurements from five to twelve can be appropriately compensated which show a sensible deviation in the cylinder pressure because of the variation of the charge air pressure. At high charge air pressures the measurement is corrected downwards and at low charge air pressures the other way round. The slight variation in charge air temperature is hardly noticeable. Generally, the simulative correction leads to an almost constant maximum pressure curve at the level of the reference measurement, even when more parameters are varied at the same time.

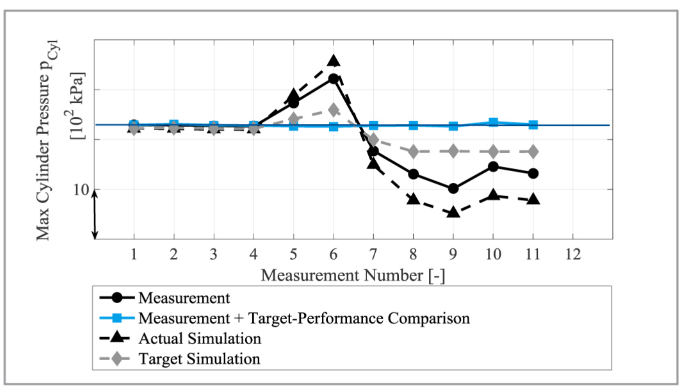

Figure 14. Pressure correction of inaccurate measurements by 0D engine simulation.

Figure 15 shows the simulative correction of the indicated engine efficiency. The meaning of the colored curves is the same as above. The shapes of the curve measured and simulated are quite similar to the pressure curve in Figure 14 since the pressure is considered in the calculation of the indicated power which is in the numerator in the equation for the efficiency indicated (see equation (16)).

$$\eta_{ind} = \frac{P_{ind}}{\dot{m}_{Fuel} \cdot LHV} \tag{16}$$

Though, it becomes obvious that the blue curve corrected still contains small deviations. The reason for this lies in the slight error of the injection duration used for the target simulation.

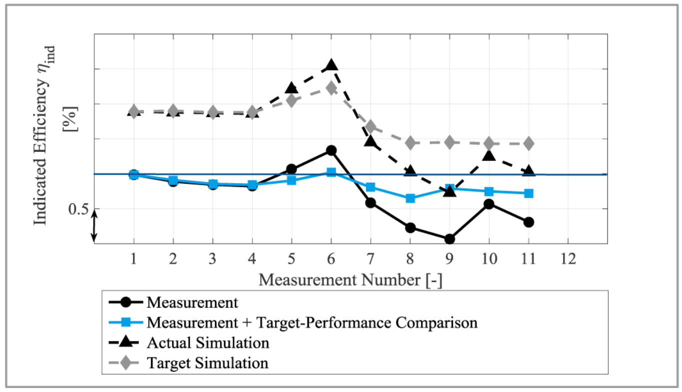

Figure 15. Efficiency correction of inaccurate measurements by 0D engine simulation.

As a result, the target simulation does not get this information the injection duration of the measurement is assumed. The efficiency measured in the first four measurements is slightly reduced compared to the corrected curve. The raised charge air temperature decreases the air density and accordingly the charge. This leads to a decrease of the maximum cylinder pressure. To ensure the constant load more fuel must be injected and the indicated efficiency decreases. At measurement five and six the charge air pressure was increased leading to an increase in indicated efficiency. This can be corrected by the simulation. Furthermore the correction of the other measurements from seven to ten shows the right trend. Because of the small failure of the injection mass used, the correction does not reach 100% accuracy. As shown, the model used for the diesel combustion also allows slight rail pressure variations to be corrected. Greater variations are not permitted since the error in the injected fuel mass is not negligible.

Figure 16 shows the correction of the specific fuel consumption. It is clear that the blue curve is closer to the dark blue line, which is the optimum solution. A high charge air pressure leads to an increase in the effective mean pressure. Hence, injected fuel mass will be reduced to ensure the constant load. This is the reason why the specific fuel consumption is corrected upwards at measurement number 6. If the charge air pressure is decreased the specific fuel consumption is simulated downwards. It becomes obvious that the curve corrected nearly matches the ideal curve.

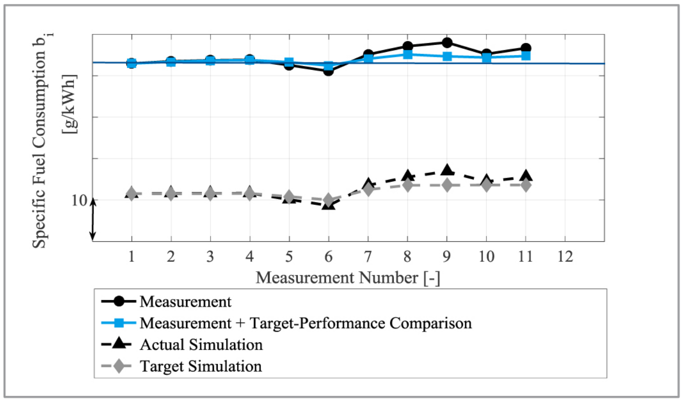

Figure 16. Correction of the specific fuel consumption of inaccurate measurements by 0D engine simulation.

Figure 17 shows the correction of the NO_x emission. In this paper the NO_x emission model according to Heider [28] is used. The actual simulation curve matches the curve simulated in its shape, but with an offset of about 250ppm. The correction does not lead to a further improvement in accuracy.

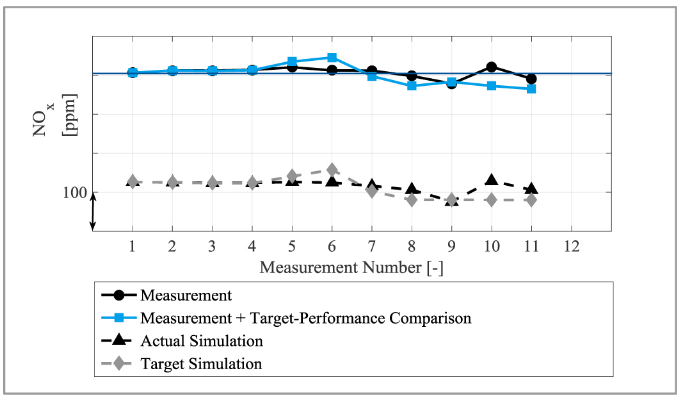

Figure 17. NO_x correction of inaccurate measurements by 0D engine simulation.

The tendency is realistic because the parameters changed lead to a decrease in combustion temperature, which implies decreasing NO_x emission. However, for an accurate correction the resolution of the used NO_x model shows a deficit and further developments in NO_x model are required.

Summary and Conclusions

In this paper an efficient methodology for engine testing was presented. The new methodology combines various methods and tools for increasing the quality and validity of measurements taken at an engine test bench to improve the process of decision making for combustion-relevant component setups and reduce the number of erroneous measurements. A stationary point detection, signal quality and plausibility checks have been utilized to ensure a high overall quality of recorded measurements. In order to ensure high measurement validity, measurement signals are continuously monitored, while a fuzzy designer checks their accuracy to avoid sensor drifts. A 0D engine simulation is used to predict the next operating point at the engine test bench and to correct slightly errors in manual input values.

All methods and tools introduced have been implemented at an industrial engine test bench for validation purposes. A measurement campaign was performed, investigating three different combustion-relevant hardware setups. In addition, special measurements were also taken in order to validate all implemented methods and tools.

This has shown that the utilization of the methods for increasing measurement quality is able to reduce the number of erroneous measurements significantly. During the measurement campaign, the percentage of invalid measurements was decreased from approximately 13% to 3%. The utilization of design of experiments is also reducing the number of measurements. Compared to full factorial test plans for industrial engine testing in recent years, statistical test plans reduce the number of measurements by about 17% within this study.

A performance comparison of the three engine hardware setups investigated showed that one hardware setup was not able to meet the defined requirements regarding NO_x and soot emissions. The other two hardware setups fulfilled all requirements. Depending on the load profile demanded by the customers, the hardware setup leading to better specific fuel oil consumption can be chosen accordingly.

The correction of small parameter deviations by 0D engine simulation gives an expedient tendency for the maximum pressure, the efficiency and thereby the specific fuel consumption in order to correct the measurement. It provides a finer resolution of accuracy for most of the target values, except emissions such as NO_x and soot. The error between the ideal and the inaccurate measurement can be reduced, leading to an increase in measurement validity. This method may therefore provide a crucial hint for decision-making when various engine components are benchmarked.

Finally, this study has helped to show that utilizing methods and tools for increasing measurement quality and validity can improve the process of engine testing. Valuable development time and costs can be saved by reducing the number of erroneous measurements, which have to be retaken.

The developed methodology is currently in use at several engine test benches of MAN Diesel & Turbo SE. After gaining experience in the day-to-day business in terms of large bore engine testing further development potentials of the methodology can be identified. Furthermore, all developed tools can be improved to meet the requirements of the users regarding usability.

References

1. Fritz, S. C., “Entwicklung und Umsetzung einer zentralisierten Messdatendiagnose für Motorenprüfstände als integrierter Bestandteil des Prüfstandssystems“, Ph.D. Thesis, Technical University of Darmstadt, Darmstadt, 2008.
2. Franze, R. M., ”Online Messdatenplausibilisierung am Motorenprüfstand“, Ph.D. Thesis, Technical University of Munich, Munich, 2011.
3. Flohr, A., “Konzept und Umsetzung einer Online-Messdatendiagnose an Motorenprüfständen”, Ph.D. Thesis, Technical University of Darmstadt, Darmstadt, 2005.

4. Wohlthan, M., Pirker, G., Krenn, M., and Wimmer, A., “LEC-Mcheck - A methodology to detect measurement errors at engine test beds“, 15th Conference “The Working Process of the Internal Combustion Engine”, Graz, 2015.
5. Friedrich, C., Auer, M., and Stiesch, G., "Model Based Calibration Techniques for Medium Speed Engine Optimization: Investigations on Common Modeling Approaches for Modeling of Selected Steady State Engine Outputs," *SAE Int. J. Engines* 9(4):1989-1998, 2016, doi:10.4271/2016-01-2156.
6. von Imhoff, B., Zweck, J., and Wachtmeister, G., "Detection of Stationary Operating States of Internal Combustion Engines," SAE Technical Paper 2015-01-1643, 2015, doi:10.4271/2015-01-1643.
7. Kötter, H., “Abschlussbericht zum FVV-Vorhaben Nr. 836: Kennfeldoptimierung - Rechnergestützte Kennfeldoptimierung. / Forschungsvereinigung für Verbrennungskraftmaschinen e.V. (FVV)“, Frankfurt am Main, 2007 (Heft 831).
8. Deflorian, M., “Versuchsplanung und Methoden zur Identifikation zeitkontinuierlicher Zustandsraummodelle am Beispiel des Verbrennungsmotors“, Ph.D. Thesis, Technical University of Munich, Munich, 2011.
9. Cao, S. and Rhinehart, R., “An Efficient Method for On-Line Identification of Steady State”, *Journal of Process Control* 5(6):363-374, 1995, doi:10.1016/0959-1524(95)00009-F.
10. Bhat, S. and Saraf, D., “Steady-State Identification, Gross Error Detection, and Data Reconciliation for Industrial Process Units”, *Industrial & Engineering Chemistry Research* 43(15):4323-4336, 2004 doi:10.1021/ie030563u.
11. Kelly, J. and Hedengren, J., “A Steady-State Detection (SSD) Algorithm to Detect Non-Stationary Drifts in Processes”, *Journal of Process Control* 23(3), 2013, doi:10.1016/j.jprocont.2012.12.001.
12. Narasimhan, S., Kao, C., and Mah, R., “Detecting Changes of Steady States Using the Mathematical Theory of Evidence”, *AIChE Journal* 33(11), 1987, doi:10.1002/aic.690331125.
13. AVL List GmbH, “AVL PUMA OPEN 2012 - Produktbeschreibung - Stationärmessung“, Graz, 2012.
14. Kristl, Seibt & Co GmbH, “Tornado - Benutzerhandbuch Tornado Designer“, Revision 1.26. Graz, 2012.
15. Brettschneider, J., “Berechnung des Luftverhältnisses λ von Luft-Kraftstoff-Gemischen und des Einflusses von Messfehlern auf λ”, *Bosch Technische Berichte* 6(4):177-186, 1979.
16. Benson, E., Zhang, Q., Reid, J., and Dickson, M., "Fuzzy Quality Evaluation for Agricultural Applications," SAE Technical Paper 2000-01-2621, 2000, doi:10.4271/2000-01-2621.
17. Mendel, J. M., “Fuzzy Logic Systems for Engineering: A Tutorial”, *Proceedings of the IEEE* 83(3):345-377, 1995, doi:10.1109/5.364485.
18. Eilts, P. and Stoeber-Schmidt, C., "Further Development and Application of a Model for the Calculation of Heat Release in Direct Injection Diesel Engines," *SAE Int. J. Engines* 7(1):120-130, 2014, doi:10.4271/2014-01-1076.
19. Pirker, G., Chmela, F., and Wimmer, A., "ROHR Simulation for DI Diesel Engines Based on Sequential Combustion Mechanisms," SAE Technical Paper 2006-01-0654, 2006, doi:10.4271/2006-01-0654.
20. Chmela, F. and Orthaber, G., "Rate of Heat Release Prediction for Direct Injection Diesel Engines Based on Purely Mixing Controlled Combustion," SAE Technical Paper 1999-01-0186, 1999, doi:10.4271/1999-01-0186.
21. Barba, C., Burkhardt, C., Boulouchos, K., and Bargende, M., "A Phenomenological Combustion Model for Heat Release Rate Prediction in High-Speed DI Diesel Engines with Common Rail Injection," SAE Technical Paper 2000-01-2933, 2000, doi:10.4271/2000-01-2933.
22. Auer, M., “Erstellung phänomenologischer Modelle zur Vorausberechnung des Brennverlaufes von Magerkonzept-Gasmotoren“, Ph.D. Thesis, Technical University of Munich, 2010.
23. Auer, M., Blodig, S., and Wachtmeister, G., “Combustion Modelling of Open Chamber and Pre-Chamber Gas Engines“, 9th Stuttgarter International Symposium, Stuttgart, 2009.
24. Walther, H. P., and Wachtmeister G., “Phänomenologisches Verbrennungsmodell für Magerkonzept-Gasmotoren mit Piloteinspritzung“, Dessauer Gasmotorenkonferenz, 2011.
25. Quérel, C., Grondin, O., and Letellier, C., "A Semi-Physical NOx Model for Diesel Engine Control," SAE Technical Paper 2013-01-0356, 2013, doi:10.4271/2013-01-0356.
26. Wilhelmsson, C., Tunestål, P., Widd, B., and Johansson, R., "A Physical Two-Zone NOx Model Intended for Embedded Implementation," SAE Technical Paper 2009-01-1509, 2009, doi:10.4271/2009-01-1509.
27. Karaky, H., Mauviot, G., Tauzia, X., and Maiboom, A., "Development and Validation of a New Zero-Dimensional Semi-Physical NOx Emission Model for a D.I. Diesel Engine Using Simulated Combustion Process," *SAE Int. J. Engines* 8(4):1924-1937, 2015, doi:10.4271/2015-01-1746.
28. Heider, G., “Schadstoffbildung II - Berechnung der Schadstoffemissionen von Dieselmotoren“, FVV-Forschungsheft 632, 1996.
29. Bayer, J. and Foster, D., "Zero-Dimensional Soot Modeling," SAE Technical Paper 2003-01-1070, 2003, doi:10.4271/2003-01-1070.
30. Fusco, A., “Application of a Phenomenological Soot Model to Diesel Engine Combustion“, International Symposium COMODIA, Yokohama, 1994.
31. International Maritime Organization, “Revised MARPOL Annex VI - Regulations for the Prevention of Air Pollution from Ships and NOx Technical Code”, 2008.

Contact Information

Christian Friedrich
Combustion Development
Advanced Engineering and Exhaust Aftertreatment
Engineering Four-Stroke
MAN Diesel & Turbo SE
Stadtbachstrasse 1, 86153 Augsburg, Germany
christian.friedrich@man.eu

Yves Compera
Institute of Internal Combustion Engines
Technical University of Munich
Boltzmannstrasse 14, 85748 Garching, Germany
compera@lvk.mw.tum.de

Acknowledgements

This study is part of the joint research project "METHODIK" supported by the Federal Ministry for Economic Affairs and Energy on basis of a decision by the German Bundestag. All responsibility for the content of this publication lies with the authors.

Supported by:

Federal Ministry for Economic Affairs and Energy

on the basis of a decision by the German Bundestag

Definitions\Abbreviations

CO - Carbon monoxide

CO_2 - Carbon dioxide

CR - Common rail

DoE - Design of experiments

ECU - Engine control unit

HC - Unburned hydrocarbons

NO_x - Nitrogen oxides

ROHR - Rate of heat release

SOI - Start of injection

SSD - Steady state detection

Nomenclature

A - Mathematical set

b_i - Indicated specific fuel consumption

i - Consecutive index

j - Numerator variable

$g_{m_{y_i}^n}$ - Gradient of the moving average of a measurement signal y_i taking n samples

g_{y_i} - Gradient of a measurement signal y_i

H_a - Absolute air humidity

$l_{g_{m_{y_i}^n}}$ - Gradient limit of the moving average of a measurement signal y_i taking n samples

$l_{g_{y_i}}$ - Gradient limit of a measurement signal y_i

$l_{O_2,Balance}$ - Oxygen mass balance limit

$l_{SNR_{y_i}}$ - Signal to noise ratio limit of a measurement signal y_i

$\dot{m}_{Air}$ - Air mass flow into the engine

$\dot{m}_{CO}$ - Mass flow carbon monoxide

$\dot{m}_{CO_2}$ - Mass flow carbon dioxide

$\dot{m}_{Fuel}$ - Fuel mass flow into the engine

$\dot{m}_{H_2O,Air}$ - Water mass flow in the air into the engine

$\dot{m}_{H_2O,Exhaust}$ - Water mass flow in the exhaust gas

$\dot{m}_{NO_x}$ - Mass flow nitrogen oxides

$\dot{m}_{O_2}$ - Oxygen mass flow in the exhaust gas

$\dot{m}_{O_2,Engine,in}$ - Oxygen mass flow into the engine

$\dot{m}_{O_2,Engine,out}$ - Oxygen mass flow out of the engine

$m_{y_i}^n$ - Moving average of a measurement signal y_i taking n samples

n - Number of samples or numerator variable

n_{Engine} - Engine speed

p_{Cyl} - Cylinder pressure

P_{ind} - Indicated engine power

LHV - Lower heat caloric value

SNR_{y_i} - Statistical signal to noise ratio of a measurement signal y_i

SPV_i - Single plausibility value of a plausibility criterion i

$SSQV_i$ - Single signal quality value of a measurement signal y_i

SSV_i - Single stationary value of a measurement signal y_i

t - Time

TPV - Total plausibility value

$TSQV$ - Total signal quality value

TSV - Total stationary value

U - Mathematical set

w_i - Weight of a plausibility criterion i

x - Element of a mathematical set

y_i - Measurement signal i

$\Delta T_{Charge\ Air}$ - Charge air temperature deviation

$\Delta p_{Charge\ Air}$ - Charge air pressure deviation

Δp_{Rail} - Rail pressure deviation

ΔSOI - Start of injection deviation

η - Engine efficiency

η_{ind} - Indicated engine efficiency

φ - Crank angle

ψ - Injection angular of an injection nozzle

μ_A - Characteristic function of an element

$\sigma_{y_i}^n$ - Moving standard deviation of a measurement signal y_i taking n samples

$\vartheta_{Exhaust}$ - Exhaust gas temperature

$\xi_{O_2,Air}$ - Oxygen mass fraction in the air

$\xi_{O_2,CO}$ - Oxygen mass fraction in carbon monoxide

ξ_{O_2,CO_2} - Oxygen mass fraction in carbon dioxide

$\xi_{O_2,Fuel}$ - Oxygen mass fraction in the fuel

ξ_{O_2,H_2O} - Oxygen mass fraction in water

ξ_{O_2,NO_x} - Oxygen mass fraction in nitrogen oxides

ISSN 0148-7191

http://papers.sae.org/2017-01-0604